

WCBP 7th annual meeting

Jan. 7-10, 2003

San Francisco, CA

Title of Talk:

Limitations and Advantages in Assessing Adenovirus Homogeneity by Laser Light Scattering and Analytical Ultracentrifugation - Measuring the Aggregation of Large Biopharmaceuticals.

Author:

Steven Berkowitz, Analytical Development, Biogen Inc., 14 Cambridge Center, Cambridge, MA 02142 and John Philo, Alliance Protein Laboratories, 3957 Corte Cancion, Thousand Oaks, CA 91360

Abstract:

The task of assessing the homogeneity of preparations of Adenovirus, an important biopharmaceutical/delivery system in gene therapy, present unique analytical challenges. In this presentation, the limitations and advantages of using analytical ultracentrifugation (AUC) and intensity and dynamic light scattering (LS) for measuring aggregation and structural homogeneity of this virus will be discussed.

Light scattering measurements carried out in this study were conducted during flow injection analysis (FIA) and ion exchange chromatography (IEC). Results obtained using a FIA system containing a post column reactor (made from teflon tubing) indicate a separation force can be generated, via hydrodynamic chromatography (HDC), which enables LS experiments to be conducted on virus samples without prior clarification. This capability avoids the removal of large Adenovirus aggregates that can occur during normal sample clarification required for conducting LS experiments. In addition, LS data gathered from FIA and IEC will highlight the importance of conducting LS measurements over a range of low angles in order to minimize intra-particle interference effects. Failure to deal with these interference effects will significantly reduce the ability of LS to detect virus aggregates.

In the case of AUC, data will be presented showing that superior information on the particle size distribution of Adenovirus is obtained by using sedimentation velocity with modern AUC analysis software. Also, AUC experiments carried out on Adenovirus using sedimentation equilibrium in a CsCl density gradient can provide additional high-resolution information about Adenovirus homogeneity.

Part I: Introduction - characterizing the homogeneity of virus particles in a Adenovirus preparation

In the field of gene therapy dynamic light scattering, DLS, (also referred to by other names such as time-dependent light scattering, intensity fluctuation spectroscopy or photon correlation spectroscopy) at a single angle (usually 90°), has become a common tool for assessing the physical homogeneity of Adenovirus preparations in terms of aggregation¹. This is achieved by combining the average diffusion coefficient determined by DLS with the Stokes-Einstein equation to obtain an average virus particle size, the average hydrodynamic radius, R_h , of an equivalent solid sphere. In this presentation it is shown, for particles the size of Adenovirus aggregates, there are important experimental issues that need to be considered in using this technique (or other LS techniques) to obtain meaningful information (see Part II, sections 1 & 8). In this study, a simple flow injection analysis (FIA) system containing a light scattering (LS) detector² has been used to address some of these issues. This LS detector can measure, at the same time, both the intensity and the time-dependence of the scattered light as a function of angle. In the case of intensity LS, measurements can be made simultaneously over a large number of angles, however, in the case of time-dependent LS, measurements can only be made at one angle (Note: for DLS, changing the detector angle on this LS detector is not that simple).

Although LS techniques can provide useful data, **when properly executed**, there are significant limits to its ability to describe the distribution of Adenovirus aggregates in a virus preparation. In deed, when one uses a single size parameter, such as R_h , as an index to assess aggregation, problems can occur. These problems result from the fact that many different aggregation distributions (which describe different populations of virus aggregates) can yield the same single average value for R_h . Hence, misleading information can be derived from LS using this approach. This can be illustrated by the following example:

A stability study where the amount of virus monomer stays constant, but the state of aggregation of the aggregated material increases with time.

In this case, R_h will increase with time due to the increase in size of the aggregated material. Such results would leave the experimenter with the impression that the amount of monomeric virus material is decreasing with time. Although DLS can provide some information which can characterize the polydispersity of a sample (via Regularization and the method of Cumulants), the precision, accuracy, and resolution of the information is not very high^{3,4}. In addition, LS is a tool that is weak in its ability to detect much smaller size particles in the presence of very large particles (see Part II, section 7). Nevertheless, when LS measurements are properly performed this technique can be very sensitive in detecting low levels of large aggregates.

As a result of the limitations mentioned above, we have sought other methods to better assess the aggregation of Adenovirus. In this study we present results for one such method, velocity sedimentation analysis in a modern analytical ultracentrifuge, AUC. Data from this method indicates the AUC can provide high-resolution distribution information that can adequately characterize virus aggregation (see Part IV, section 1). Furthermore, sedimentation equilibrium experiments in a self-generating CsCl density gradient in a AUC can also provide information on other forms of Adenovirus structural polydispersity, such as density micro-heterogeneity, due to differences in the protein to nucleic acid ratio between virus particles, (see Part IV, section 2).

Part II: Light scattering (LS) experiments on Adenovirus

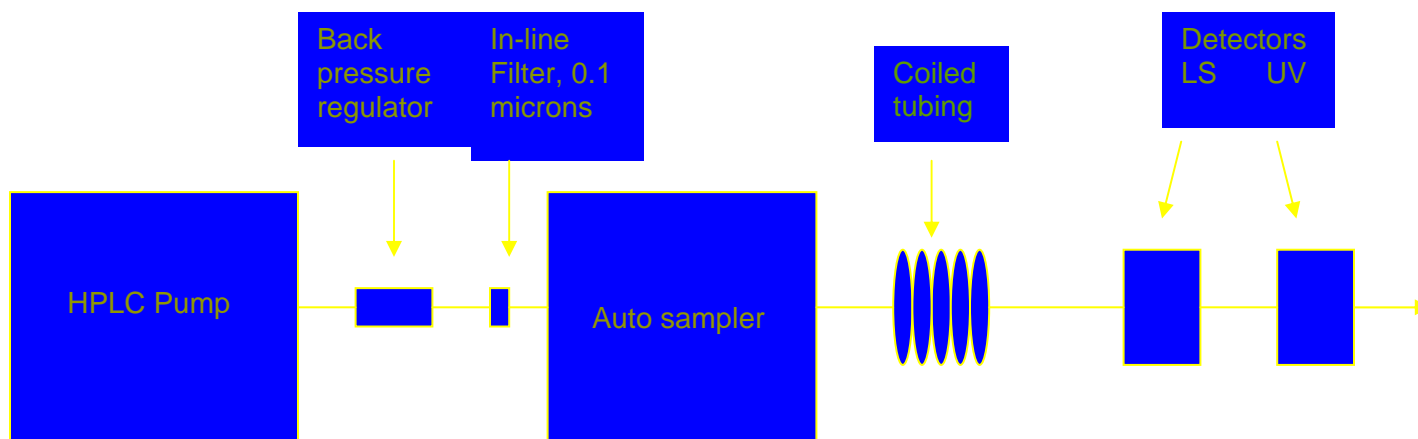
1. Issue 1 - Sample clarification and the “Dust Problem in LS”

In conducting dynamic or intensity LS experiments, a key issue is the removal of large extraneous material (which is commonly referred to as the “Dust Problem in LS”) in order to properly characterize a sample. This is achieved by a sample clarification step using either centrifugation or filtration, just prior to conducting the LS measurement.

Unfortunately, for molecules the size of Adenovirus (which is an icosahedron shape virus having a diameter close to 100 nm) and larger, such clarification can lead to the removal of material responsible for the sample’s polydispersity (see results in Part IV, which show how easy Adenovirus aggregates can be removed by centrifugation). As a result, all Adenovirus LS measurements in this work were conducted on samples that were not

clarified (samples were run “as is”). Hence to overcome the potential “Dust Problem”, LS measurements were carried out on a HPLC system using flow-injection analysis (FIA), see Figure 1. Measurements conducted on this system involved replacing the HPLC chromatography column with a long piece of teflon tubing woven in a tight serpent configuration, see Figure 2 which shows an example of the woven teflon tubing pattern (Note: this is nothing more than a post column reactor). If the mobile phase in the FIA system is run slowly enough (e.g. flow rate = 0.2 mL/min.) a separation force can be generated via hydrodynamic chromatography (HDC)^{5,6}. By taking advantage of this hydrodynamic separation, very large extraneous “Dust” particles (micron size and above) can be separated from the much smaller soluble aggregates and monomeric particles. As a result, the LS signal from the different virus species and very large extraneous particles (which might actually be very large virus aggregates themselves) can be separately detected and evaluated. Figures 1 & 3 below provide a brief schematic and description of this flow injection system and the HDC separation mechanism. Real examples, which illustrate the separation capability of this FIA system, are shown in Figure 4.

Figure 1 Flow Injection Analysis System Capable of Providing Hydrodynamic Chromatography



Mechanism of separation in Hydrodynamic Chromatography – Due to the velocity profile of the mobile phase within the teflon tubing (50' x 0.01" ID x 1/16" OD) and steric effects (due to a particle's size) which restrict large particle to the highest values of the velocity field, large particles will move faster through the tubing than smaller particles. Hence they will elute first. Note: large particles may also experience a hydrodynamic lift into the higher velocity field.

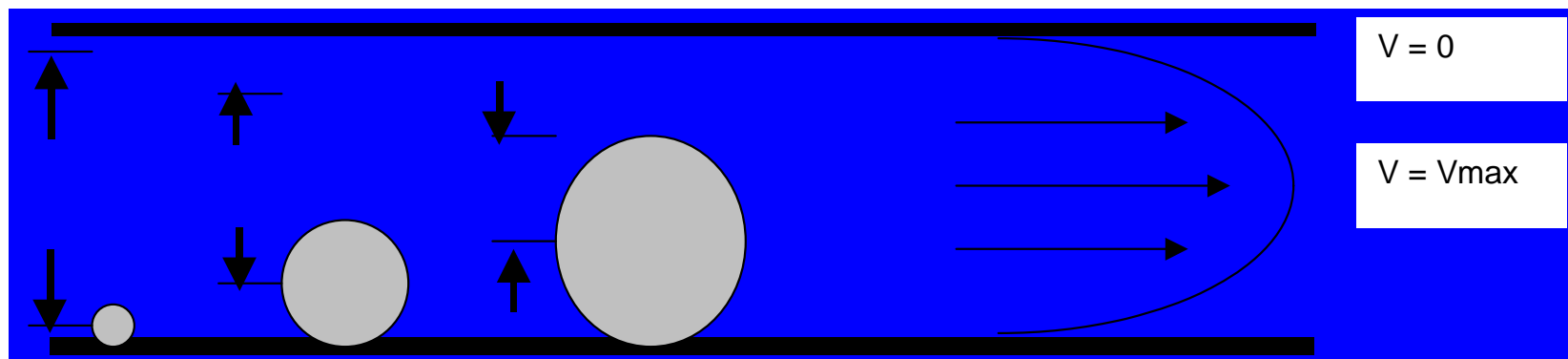


Figure 2

Serpentine Coiled Teflon Tubing

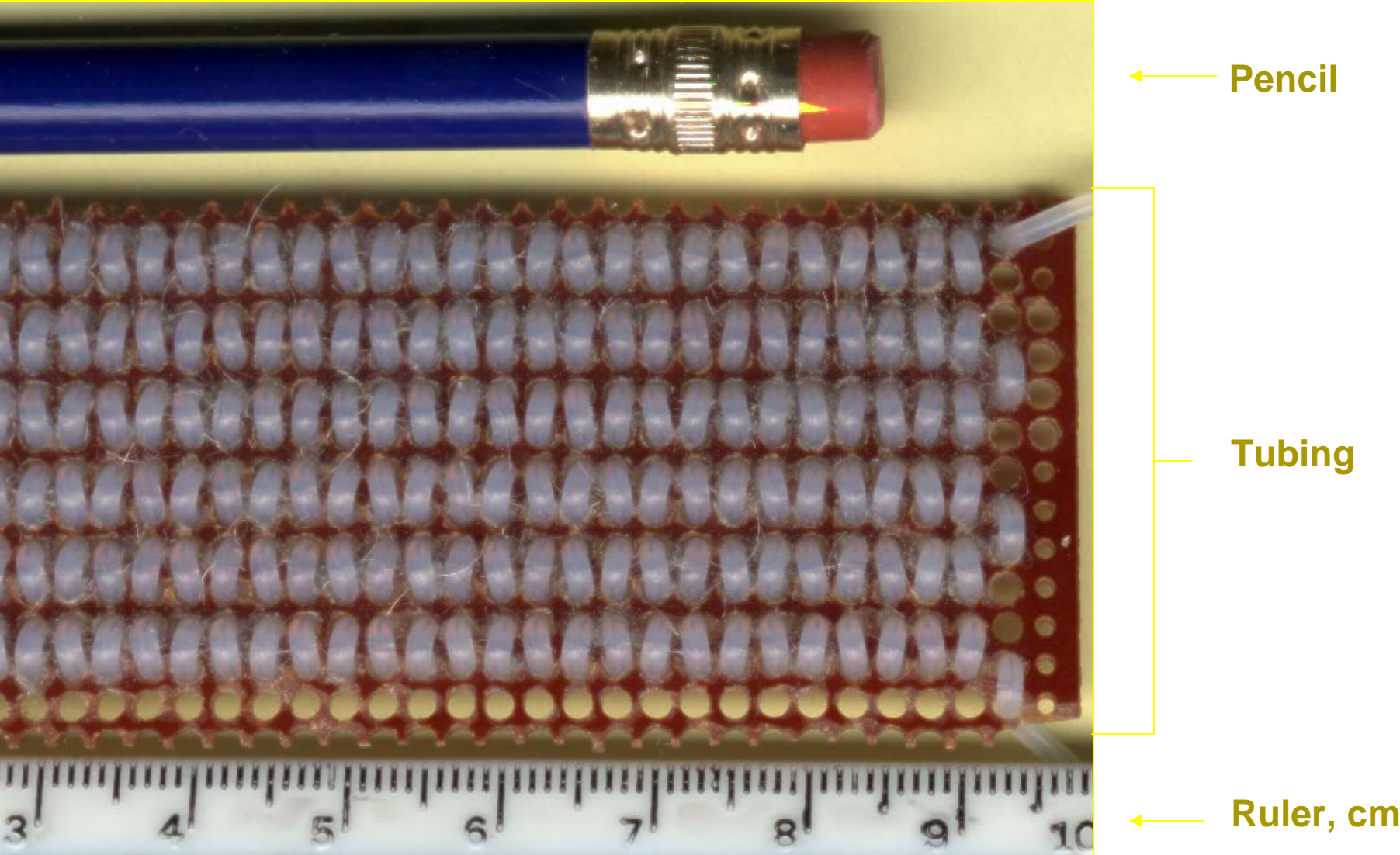


Figure 3 Operation of the FIA System with LS Detection

This figure illustrates how the FIA system shown in Figure 1 can be used to provide a "Dust-Free" sample solution and at the same time allow for the detection of particulate material or very large aggregates in a non-clarified sample during on-line LS measurements.

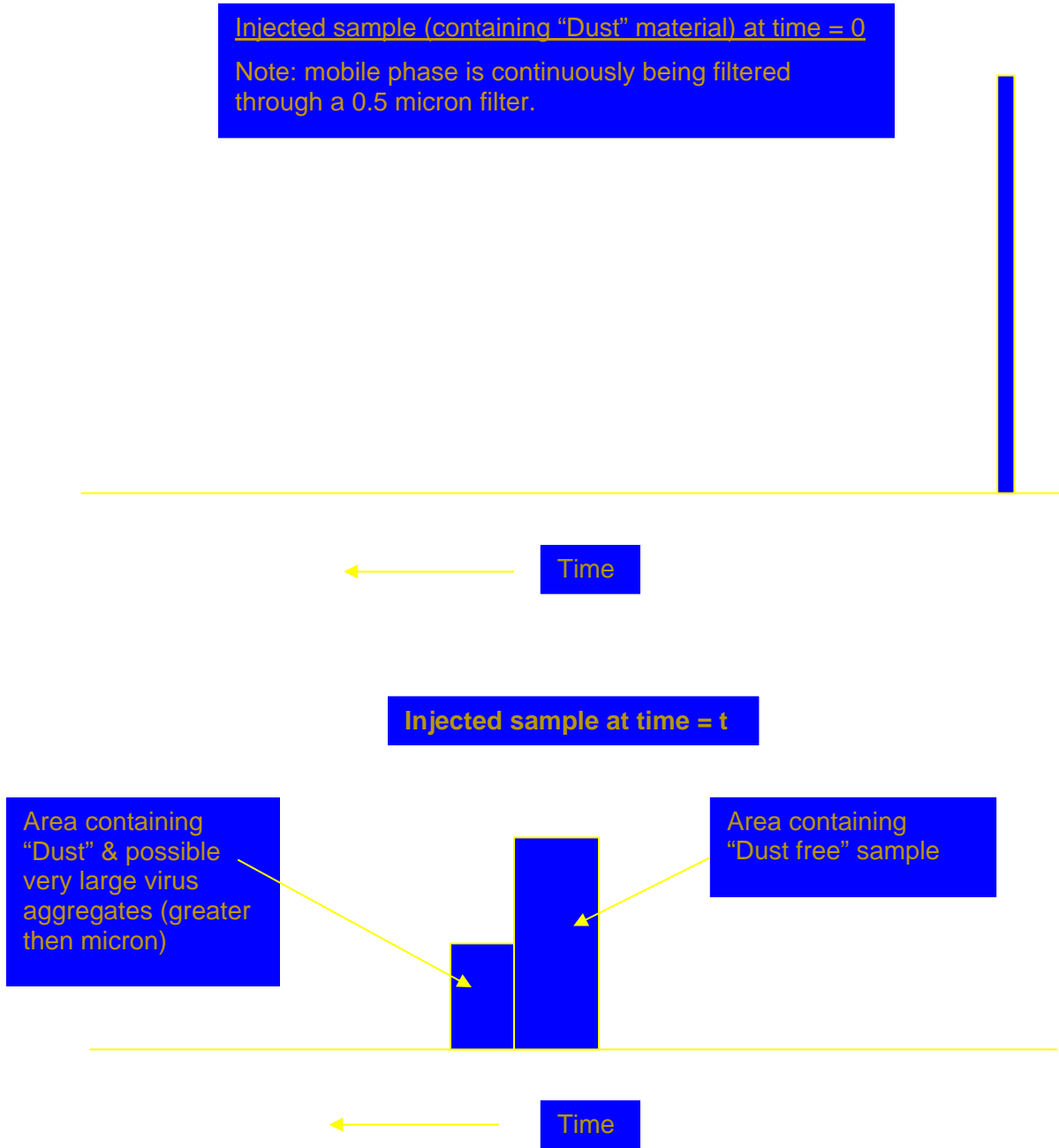


Figure 4a Difference in the Migration Time of Highly Aggregated Empty Adenovirus Capsids and a Typical Adenovirus Sample.

Overlay of the 90° LS signal from two separate flow injection analysis runs: A) typical Adenovirus preparation and B) aggregated preparation of empty Adenovirus capsids.

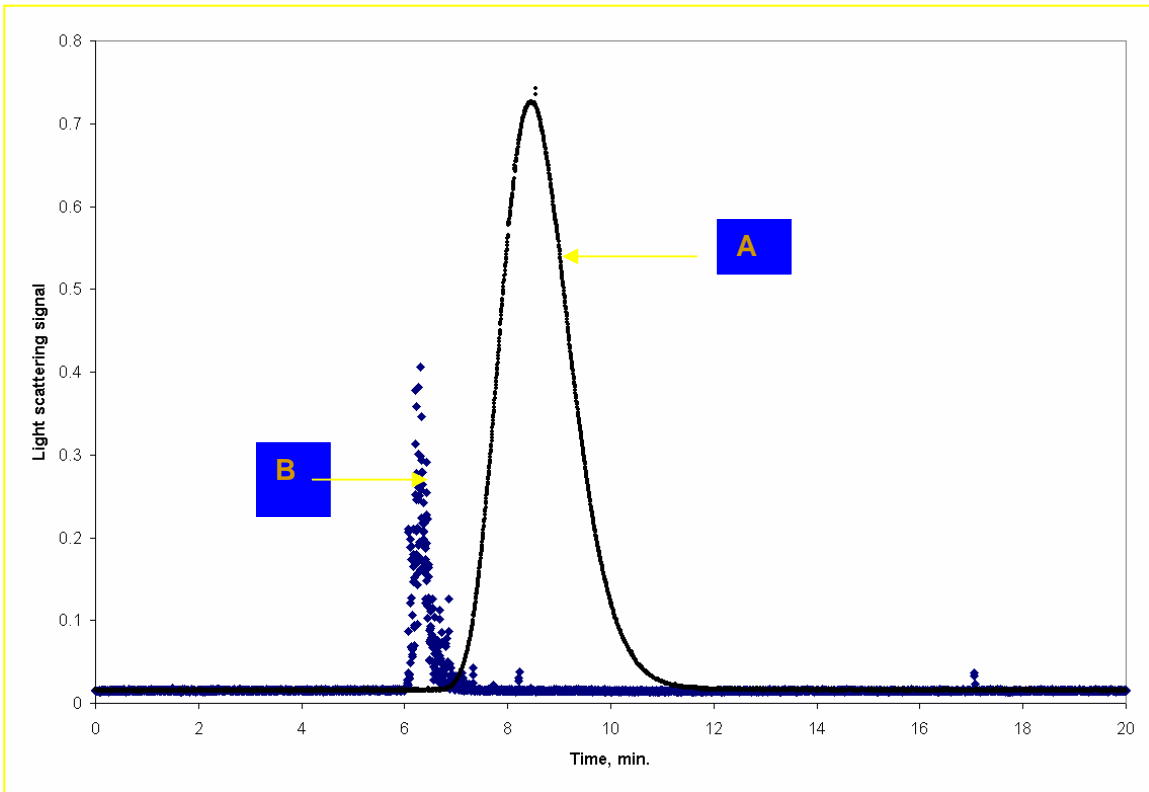


Figure 4b Flow Injection Analysis of an Antibody Stability Sample Stored at 40°C and Run “As Is”

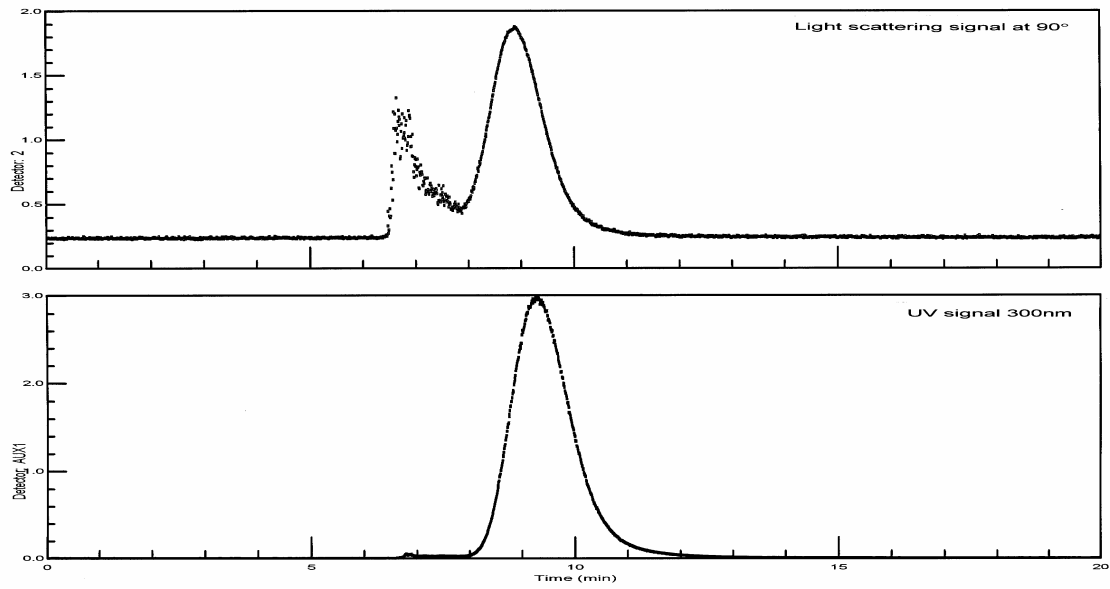
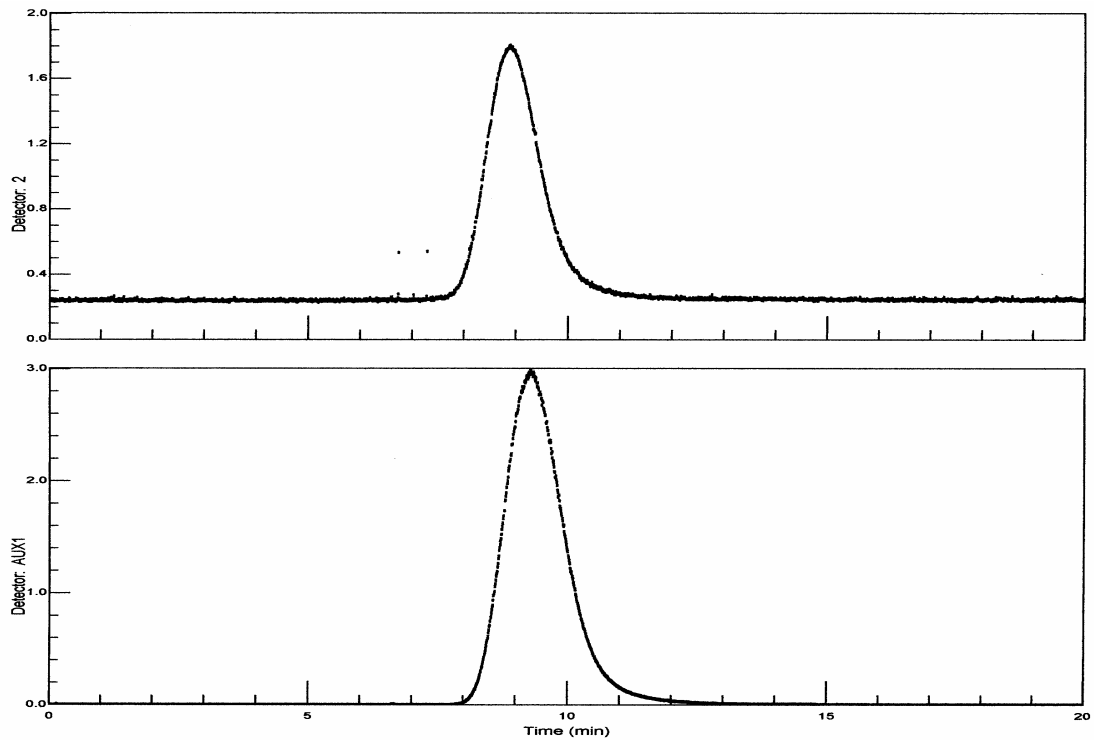


Figure 4c Same as Figure 4b but Clarified by Centrifugation



2. Results obtained by FIA on Adenovirus with UV and LS detection

Chromatograms obtained by injecting samples of Adenovirus into the FIA system discussed above, using the *Adenovirus formulation buffer as the mobile phase, in both the flow and stop-flow modes, are shown in Figures 5-6, respectively (see discussion in section 6 as to why stop-flow measurements were made). Results from these types of experiments have not revealed any signs of very large extraneous particles (particulate or insoluble material) in these virus samples, as seen in the examples shown in Figure 4. Hence, virus aggregates that are present are most likely smaller than a micron.

Values for the average particle size parameters R_h and R_{eq} (see bottom of Table 1 for the definition of this latter term) generated from the LS measurements made during FIA, are found to be significantly greater than accepted radius for the capsid of Adenovirus, which has been determined to be $43.1 \pm 2.7 \text{ nm}^7$, see Table 1. This difference is especially true for R_{eq} . In the case of the R_h value from dynamic LS, the large value could be accounted for by the presence of fiber spikes on the virus capsid particle⁸. Nevertheless, the observed larger value for R_{eq} relative to R_h is surprising given the presence of these thin fiber spikes that project out of the 12 vertices on the Adenovirus capsid. These spikes should make the value for R_h (determined from the virus' hydrodynamic properties measured by DLS), if anything, larger than the R_{eq} value (which is reflective of the distribution of mass of the virus particle measured by intensity LS measurements). This outcome arises from the stronger influence of these fiber spike projections on the virus' hydrodynamic properties relative to its minor influence on the distribution of the mass of the virus. In section 8 we will show that the large experimental observed discrepancy between R_{eq} and R_h (seen in Tables 1 & 2) results from the fact that DLS measurements were only made at one high angle (which in this study was at 111°).

*Formulation buffer - contains high glycerol and low mM buffer concentration. Unless stated otherwise all Adenovirus samples were analyzed in this buffer system.

Figure 5 Flow Injection Analysis (FIA) of an Adenovirus Preparation in the Flow Mode.

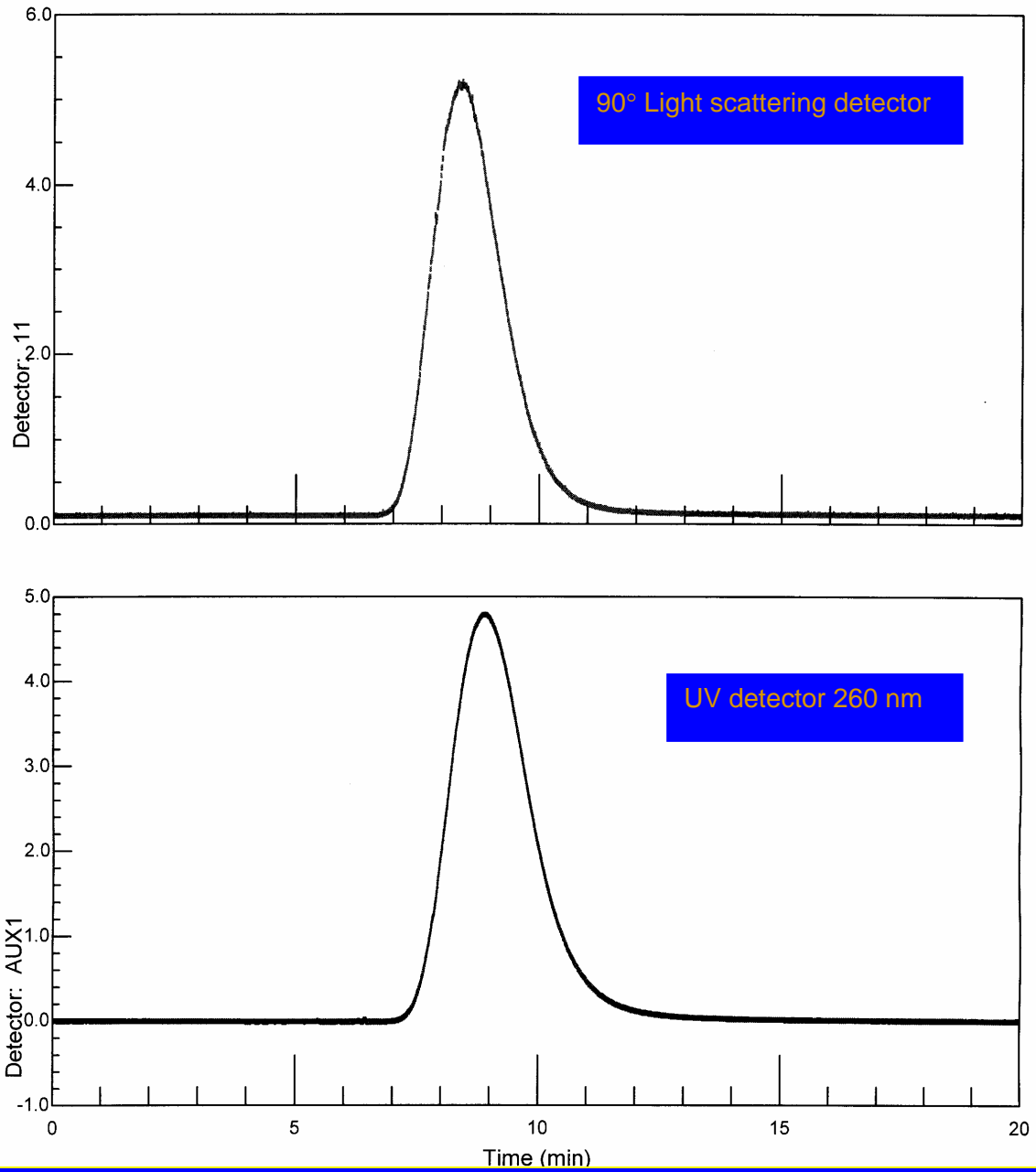
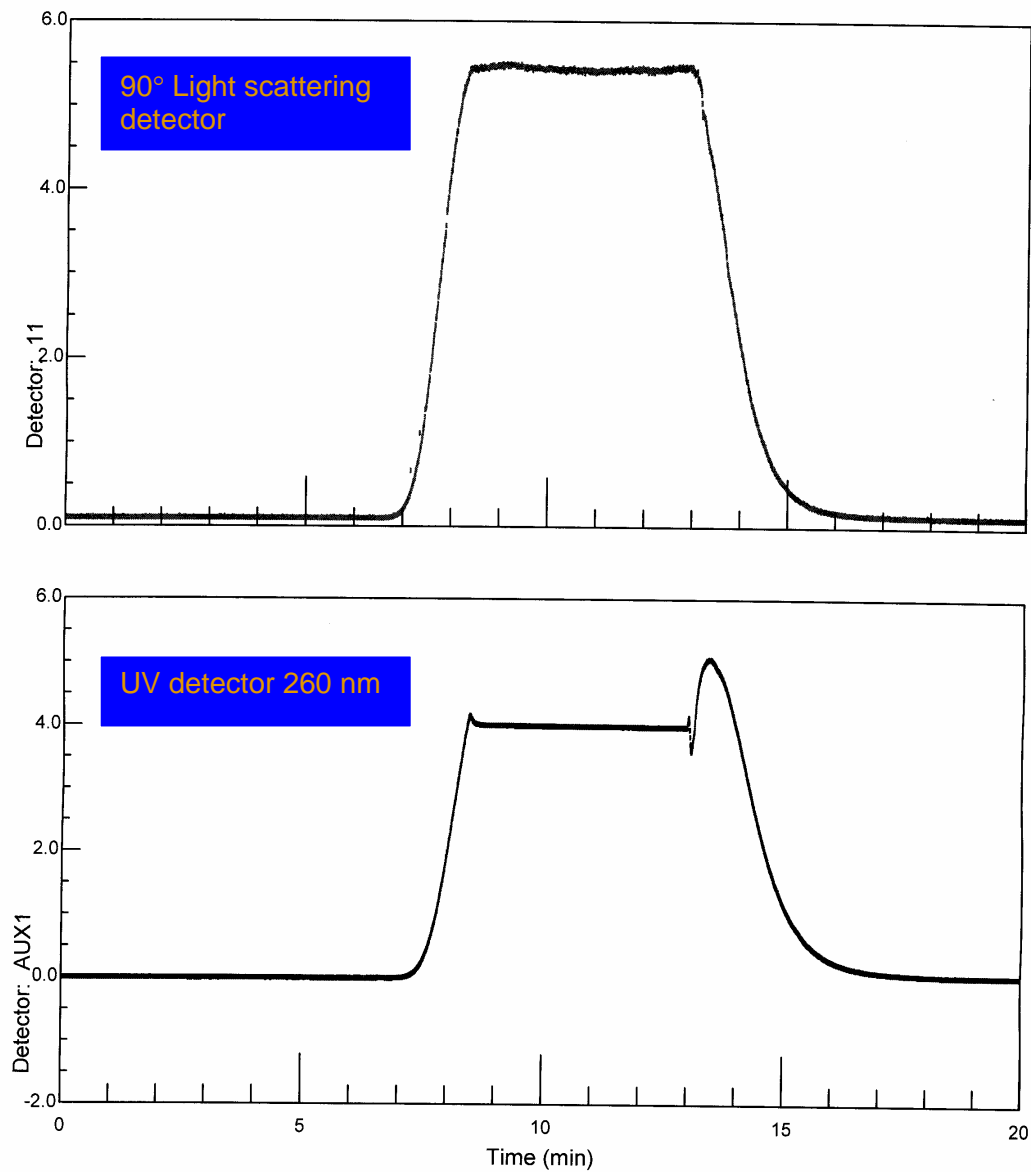


Figure 6 Flow Injection Analysis (FIA) of an Adenovirus Preparation in the Stop-Flow Mode.

Flow was stopped at the peak max. of the LS signal. Particle size information was then calculated from data collected (while the mobile phase flow was zero).



St

Table 1

Particle Size Information on a Lot of Adenovirus from LS Measurements Conducted during FIA & IEC

Sample ID	R _{rms} , nm	R _{eq} , nm	R _h , nm
Formulation buffer FIA (flow)	60	78	50
Formulation buffer FIA (stop-flow)	59	76	53
IEC (flow)	32	42	40
IEC (stop-flow)	31	41	50

R_{rms} is the root mean square radius obtained from intensity LS measurements (limiting slope at 0°)

R_{eq} is the equivalent radius for a solid sphere - $(R_{rms}^2)^{1/2} = [(3/5)(R_{eq}^2)]^{1/2} = R_g$

R_h is the hydrodynamic radius of a solid sphere with a diffusion coefficient equal to that measured by DLS.

3. Results obtained by Ion-exchange chromatography (IEC) on Adenovirus with UV and LS detection

When IEC, with on-line LS detection (using the same LS detector used in FIA experiments) was conducted on the same virus preparation, see Figure 7, used in the FIA experiments discussed above, the measured value for R_{eq} was significantly reduced, see Table 1. (Note: see section 6 as to why the R_h results obtained by DLS during IEC differs in the flow versus stop-flow modes).

Comparison analysis of the IEC intensity LS data with theoretical model calculations, discussed in section 4 below, has shown that the Adenovirus which elutes from the IEC column is monodisperse with a particle diameter of about 90 nm. This result agrees well with the diameter for the Adenovirus capsid (reported for the Adenovirus reference standard, ARM, developed by the Adenovirus Reference Material Working Group, ARMWG) of 86.2 nm ⁷.

4. Comparison of experimental intensity LS data measured for the Adenovirus IEC peak, with theoretical intensity LS data calculated for solid spheres of different sizes (diameters).

The intensity of light scattered from a monodisperse sample, $I(\theta)$ as a function of angle (for vertically polarized incident light) is given by the following equation:

$$I(\theta) = K c M P(\theta) \quad \text{eq. 1}$$

Where:

K = a collection of constant terms

c = is the concentration of the molecules with a molecular weight M

$P(\theta)$ = the particle scattering or form factor (which for large scatterers like Adenovirus and its aggregates accounts for the intra-particle interference effects and hence the angular dependence of the observed scattered light for a molecule having particular size & shape).

If the LS experiment is conducted at low enough concentration, on molecules whose size is comparable or larger than the wavelength of the incident light, information about the size and shape of those molecules can be obtained by studying the angular dependence of $P(\theta)$. One way of achieving this is to compare the experimental $P(\theta)$ data with theoretical $P(\theta)$ data calculated from equations that can model the angular dependence of the scattered light from molecules of known shapes and sizes. One such model is a solid sphere:

$$P(\theta)_{\text{solid sphere}} = [(3/x^3)(\sin x - x \cos x)]^2 \quad \text{eq. 2}$$

Where:

$$x = [(2\pi D / \lambda) \sin (\theta/2)]$$

D = Diameter of the solid sphere

λ = Wavelength of the incident in the buffer solution

The scattering of light from a solid sphere represents a good theoretical model to account for the light scattered from an Adenovirus capsid since scattering from the fiber projections can be ignored because of its small mass relative to the large total mass of the virus capsid. If an Adenovirus preparation is monodisperse we can use eq. 2 to calculate the theoretical angular dependence of the LS data for different spheres and compare it with experimental data. By carrying out this comparison the actual size of the Adenovirus monomer particle in solution can be determined using all of the angular intensity LS data. Such an approach provides more confidence in the measured R_{eq} value relative to the R_{eq} value determined from the limiting slope at $\theta=0^\circ$ using various extrapolation procedures for Zimm, Debye, or Berry plots.

In order to conduct a direct comparisons between experimental data and theoretical calculations, the calculated scattering factors (as a function of angle), for spheres of different diameters, were converted to normalized scattering factors, $P_n(\theta)$, using equation 3:

$$P_n(\theta) = P(\theta)/P(90^\circ) \quad \text{eq. 3}$$

Similarly, experimental Adenovirus LS values for $I(\theta)$, obtained during IEC, were also converted to normalized scattering factors by combining eqs. 1 & 3:

$$P_n(\theta) = P(\theta)/P(90^\circ) = I(\theta)/I(90^\circ) \quad \text{eq. 4}$$

The resulting normalized theoretical data were then plotted to generate theoretical normalized LS envelopes, see Figure 8. By comparing these theoretical calculated scattering envelopes, for solid spheres of different diameters, with the plot of the experimental normalized LS envelope obtained for Adenovirus IEC peak, an excellent match was observed between the experimental plot and the theoretical plot for a solid sphere having a diameter of 90 nm (or a radius of 45 nm), see Figure 8. This radius is very close to the radius reported by the Adenovirus Reference Material Working Group (ARMWG) for the monomeric Adenovirus Reference Material (ARM) capsid of 43.1 nm⁷. Hence the eluting virus peak from the IEC experiment is monodisperse. This conclusion is also supported by the results shown in Figure 9, which indicates that the particle size, R_{rms} (see Table 1 for definition of this term), across the eluting IEC peak is constant. Hence the decrease in the average virus particle size in passing it through an IEC column supports the conclusion that the virus sample placed on the IEC column actually contained aggregated virus material. This is also apparent when one compares the normalized LS envelope obtained for the IEC Adenovirus load to the eluted virus peak, see Figure 10 (as well as Figure 14 which shows AUC results of the same sample loaded on the IEC column, that indicates it contains only about 60% monomeric virus material). What is also significant about the data in Figure 10 is that for angles above 80° there is little difference in the observed normalized LS envelope for these two adenovirus preparations. The significance of this observation is discussed in section 8.

Based on the above data, the IEC column either separates (removes) the aggregated Adenovirus from the monomeric virus particles or during IEC chromatography the high salt, required to elute the virus off the IEC column, actually dissociates the virus aggregates. Evidence in section 5 indicates the latter may be correct the answer.

Figure 7 IEC chromatograms from the LS and UV detectors for Adenovirus

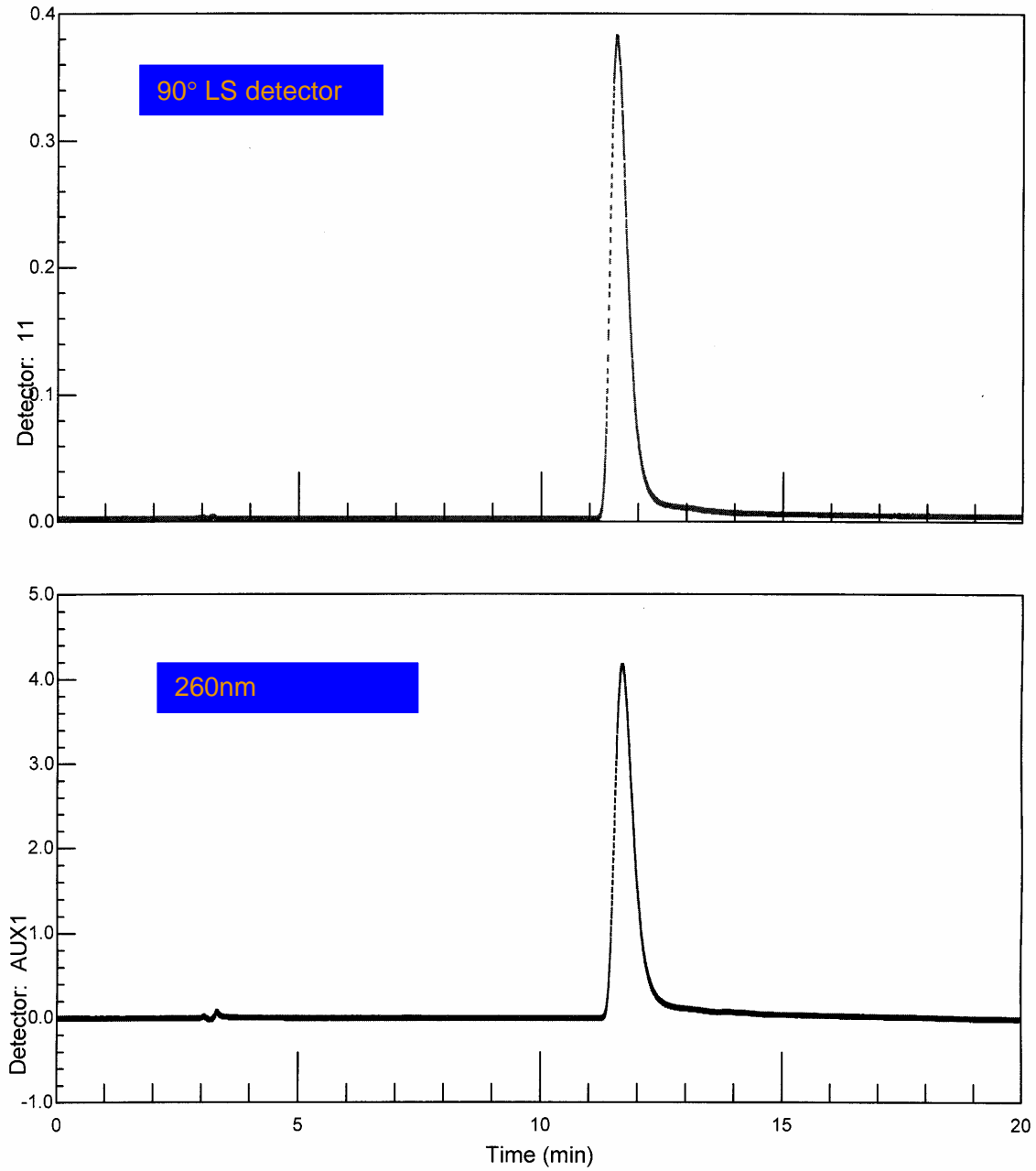


Figure 8 Comparison of the Normalized LS Envelope of Adenovirus IEC Elution Peak with the Normalized LS Envelopes from Solid Spheres of Diameters 70 - 120nm (in Steps of 10nm)

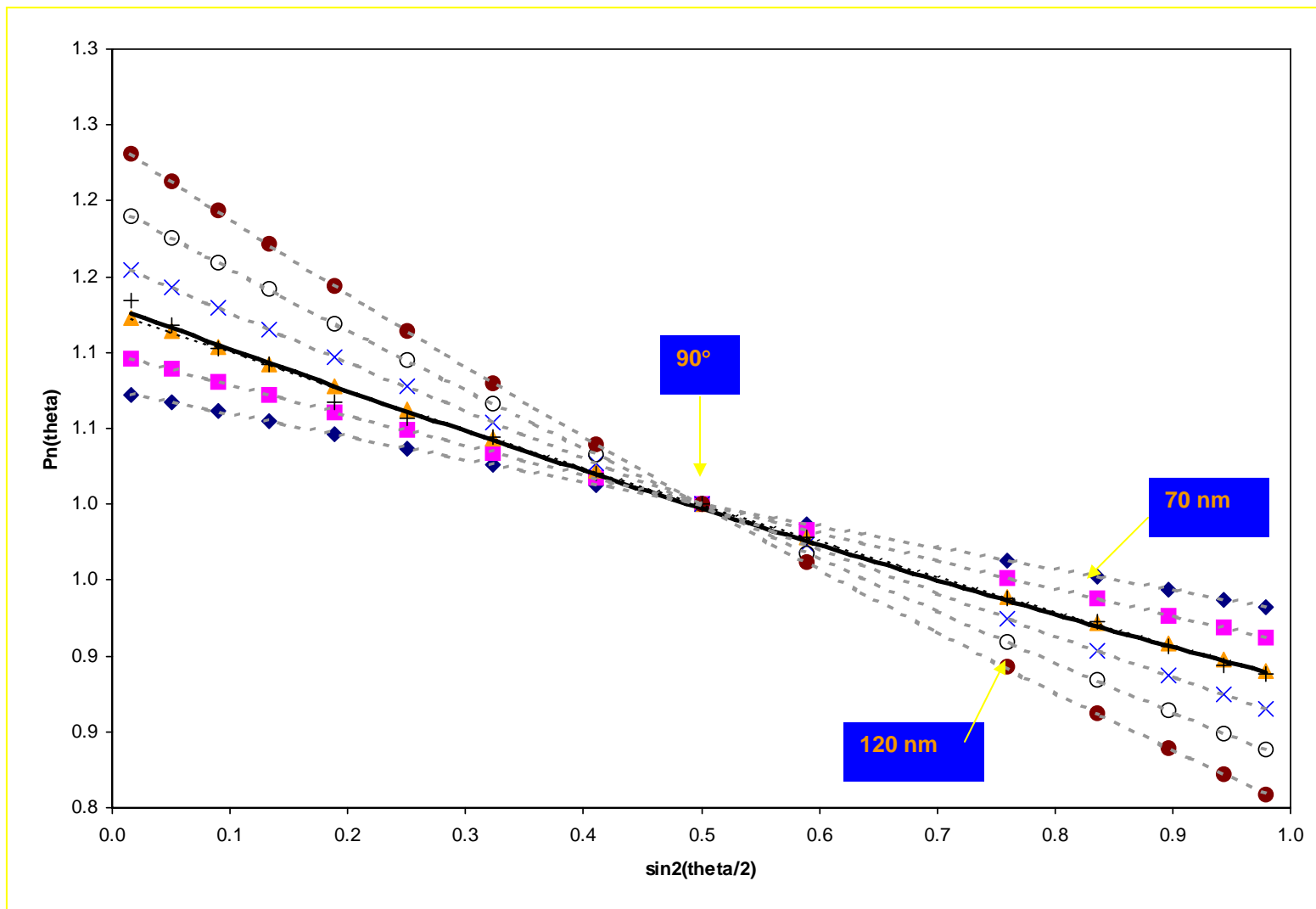


Figure 9 Calculated R_{rms} (from Intensity LS) Values Across the Adenovirus IEC Elution Peak

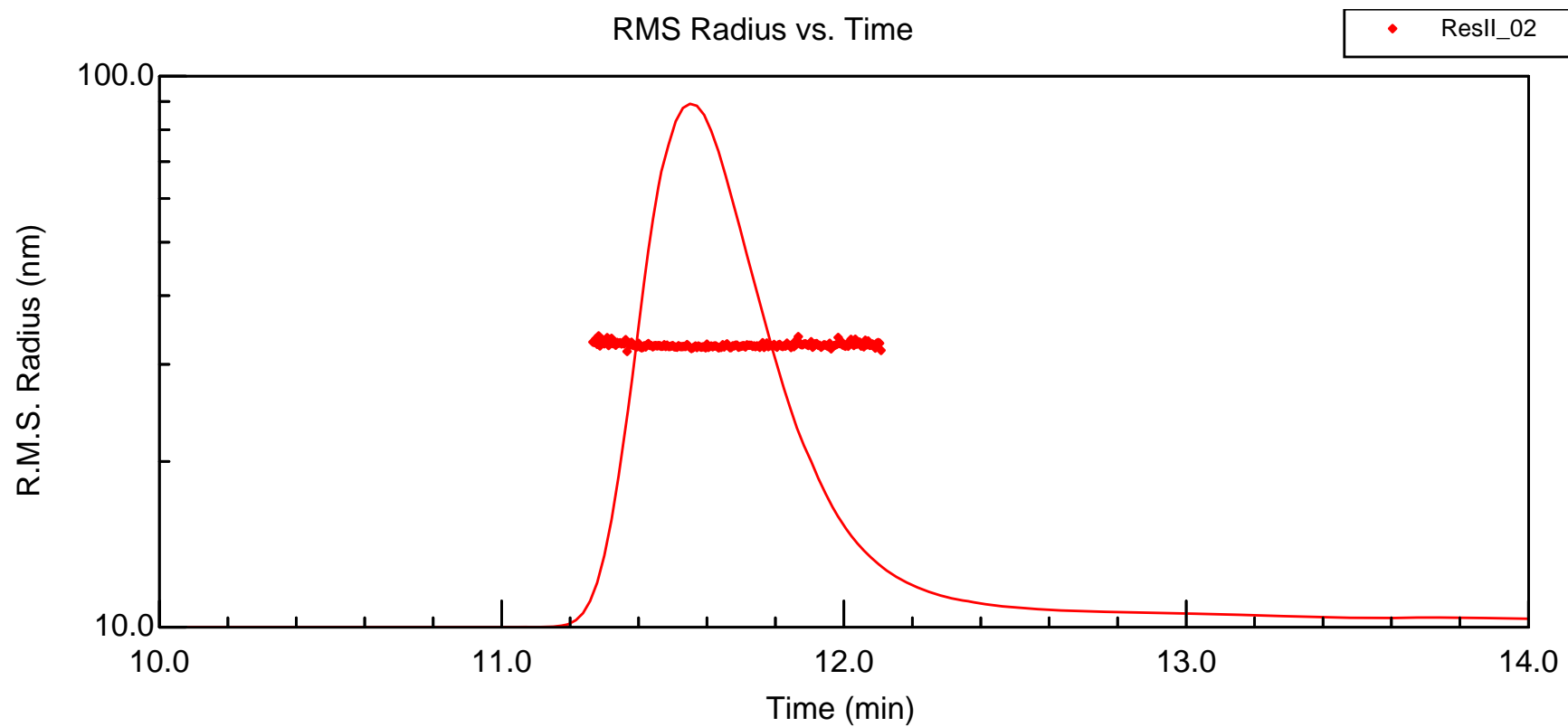
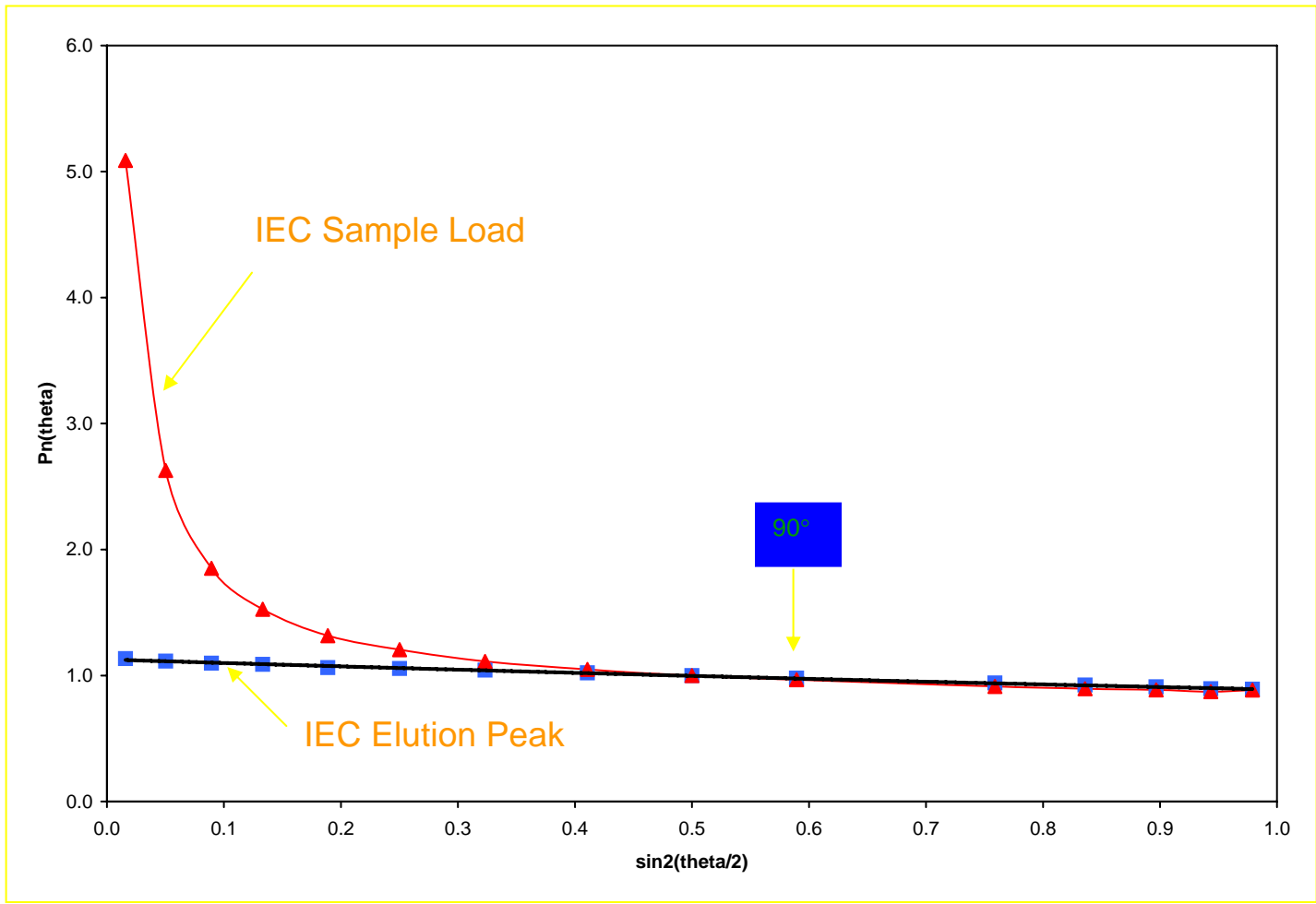


Figure 10 Normalized LS Envelope for Adenovirus IEC Sample Load vs Elution Peak



5. Evidence that the observed reduction in the average particle size of Adenovirus during IEC is due to the dissociating effect of high salt in the eluting buffer.

FIA experiments conducted on the same Adenovirus material, run in a mobile phase containing the formulation buffer with 0.5 M NaCl has also showed a reduction in the average size of the virus particle relative to that obtained by FIA for the same sample run in its normal (glycerol containing, low salt) formulation buffer. In addition, the absence of any significant flow-through peak and the absence of any other elution peak in the IEC chromatogram, other than the main virus peak (even after the use an elution gradient which went as high as 1 and 2 M NaCl), indicates the absence of a separation of the aggregated virus from the monomeric virus elution peak, see Figure 7. An even more striking result which shows the effect of high salt on Adenovirus aggregation can be found when the same experiments was carried out on a highly aggregated lot of Adenovirus (purified by CsCl density gradient and stored in the same formulation buffer, but at a much higher concentration), see Figures 12-13 and Table 2.

From the above data we have concluded that the resulting reduction in virus size, during IEC, is mostly likely due to the disassociating effect of the high salt rather than from the actual removal of stable aggregated material by IEC (also see analytical ultracentrifugation results in Figures 15-16, Part IV, section 1).

6. Limitation in determining average particle size via dynamic LS in a flow mode

Stop-flow measurements have been conducted in this study in order to evaluate the dynamic LS unit's ability to accurately measure particle size under the flow conditions used for FIA and IEC. Results obtained for FIA show no significant effect while IEC result does (see Table 1). In the latter case it appears that for particles the size of Adenovirus and larger, the higher flow rate and sharper eluting peak yield a rate of change in Adenovirus particle concentration which partially overlaps the time dependence of the decay process of the autocorrelation function for this virus and its aggregates. As a result, accurate R_h values cannot be obtained in the flow mode used in this study to conduct IEC measurements.

7. Limitation of LS methods to detect small molecules in the presence of very large particles.

The amount of light scattered as a function of angle by a monodisperse sample of spherical molecules, whose largest size is much smaller than the wavelength of the vertically polarized incident light, is given by eq. 1 where $P(\theta) = 1$ due to the small size of the molecule. This results in eq. 5 below:

$$I(\theta) = K c M \quad \text{eq. 5}$$

Since scattering from this sample comes from small molecules of the same size, DLS will yield a diffusion coefficient and therefore R_h which accurately describes the size of the sample molecule. In addition, R_h will be independent of angle. This independence of angle will also apply to scatterers whose largest dimension is comparable or bigger than the wavelength of the incident light, so long as the sample is homogeneous. However, if the sample is polydisperse, the total light scattered as a function of angle is now given by eq. 6 below:

$$I(\theta) = K \sum c_i M_i \quad \text{eq. 6}$$

Where:

c_i = Concentration of specie i

M_i = Molecular weight of specie i

This equation indicates that very large mass molecules will dominate the observed LS signal making it difficult, if not impossible, to detect the presence of much lower molecular weight molecules in the presence of much larger molecules. This can be illustrated by the following:

If a solution contains two types of molecules of equal concentration, but differ in their molecular weight by a factor of 100, and if the signal to noise ratio of the LS signal is 100, LS measurements on this sample would experimentally indicate that this sample is homogeneous since the LS signal from the much lower mass molecules would be effectively buried in the background noise.

8. Issue 2 – The reduced ability of LS methods to detect large particles in polydisperse samples when using only a single (high) angle measurement.

Finally, if the polydisperse sample also contains spherical molecules whose size is comparable to the wavelength of the incident light, the total light scattered as a function of angle is given by eq. 7:

$$I(\theta)_i = K \sum c_i M_i P(\theta)_i \quad \text{eq. 7}$$

Where:

$P(\theta)_i$ = particle scattering or form factor of specie i , whose values range from 1 (for particles much smaller than the wavelength of the incident light) to 0 (for particles much larger than the wavelength of the incident light). This parameter accounts for the reduction in scattered light as a function of high angle due to internal interference effects.

Eq. 7 indicates that if LS measurements are not conducted at low enough angle, light scattered from very large molecule can be significantly reduced or worst go undetected. Hence under these conditions LS measurements will yield particle size information that is biased towards the smaller size material.

In the case of Adenovirus and its aggregates the large size of these particles, especially Adenovirus aggregates require the use of eq. 7. As mentioned in section 4, for scatterers of known specific shape and size, exact functions for $P(\theta)$ are known. Since Adenovirus can be well approximated by a solid sphere, we can calculate the angular dependence of the intensity of the scattered light by using eq. 2, as was done in section 4. Similarly, if we approximate the Adenovirus aggregates as equivalent solid spheres of different diameters, we can also estimate the effect of angle on the resulting scattering observed for these spherical aggregates. Figure 11 shows the results for these theoretical calculations of $P(\theta)$ for homogeneous preparations of solid uniform spheres having diameters of 100, 200, and 400 nm, as a function of angle. These calculations indicate that in order for the LS instrument to effectively see the true scattering from large Adenovirus aggregates (whose dimension approach or exceed that of a sphere

having a diameter of 400 nm), LS measurements need to be carried out at low angles⁹. This point is also experimentally illustrated by data shown in Figures 12-13 and Table 2, on a lot of Adenovirus that was highly aggregated.

Unfortunately, as mentioned in the introduction, most DLS measurements conducted in the gene therapy field are carried out on instruments that have only one angle, 90°¹. Even if the instrument is capable of measuring the light scattered at other angles, reported data typically state that the average virus particle size was obtained from a single angle measurement at 90°¹. The impact of these LS measurements at a single (relatively high) angle on Adenovirus is shown in Tables 1 and 2. Data in these tables indicate that R_h values from DLS are significantly lower than the R_{eq} values obtained from the low angle intensity LS measurements (when aggregated Adenovirus was present). In this study all DLS measurements were conducted at 111°. Hence the low DLS results for R_h relative to the intensity LS results for R_{eq} (which incorporates a range of light scattering readings at different angles down to 23°) is to be anticipated.

Clearly, failure to make LS measurements at significantly low enough angle will yield information that can significantly underestimate the level of virus aggregation present and therefore underestimate the virus sample's polydispersity⁵.

Figure 11 Particle Scattering Factors for Solid Spheres Having Diameter of 100, 200, & 400 nm as a Function Angle – the Resulting Plots Represent the LS Envelope for These Spheres

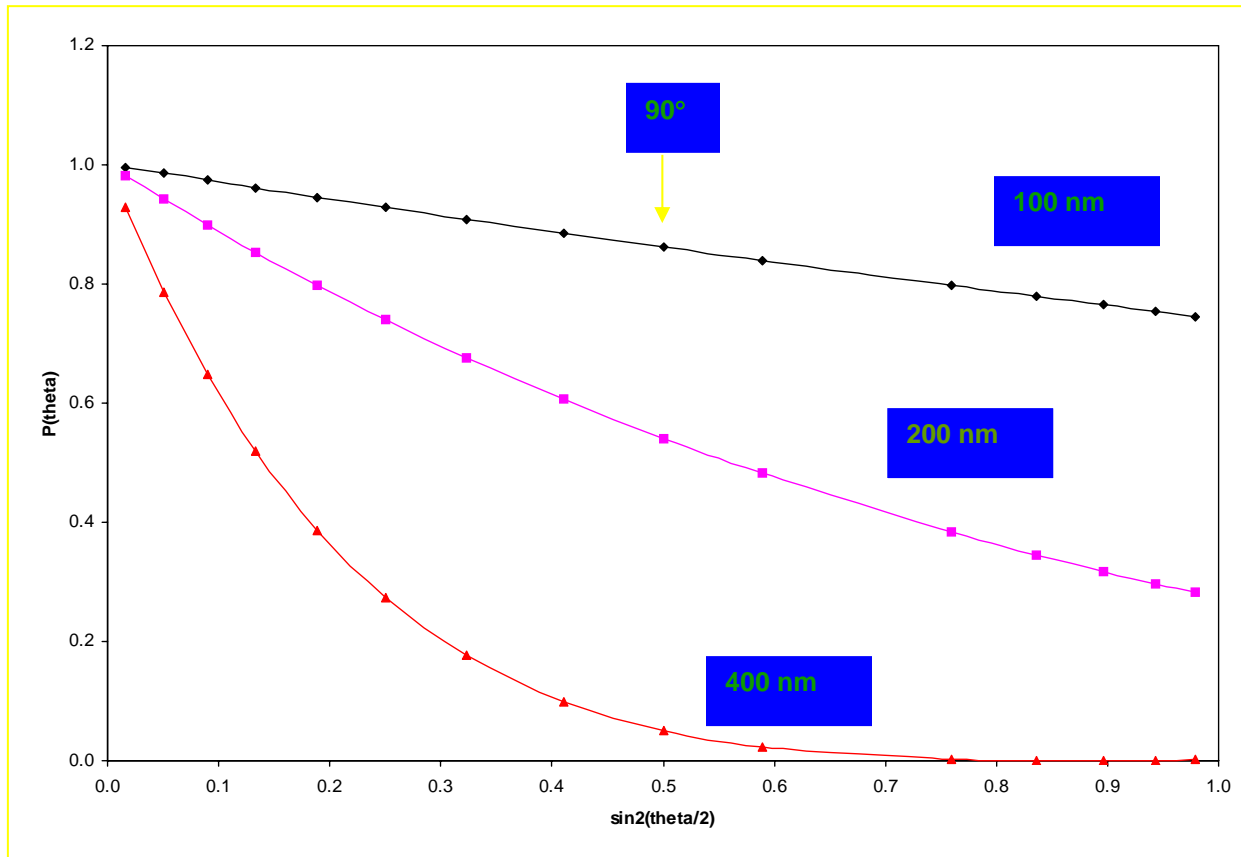


Figure 12 Comparison of the Normalized LS Envelope for a Highly Aggregated Preparation of Adenovirus to the Peak Normalized LS Envelopes for the IEC Adenovirus Sample Load & Elution Peak Shown in Figure 10.

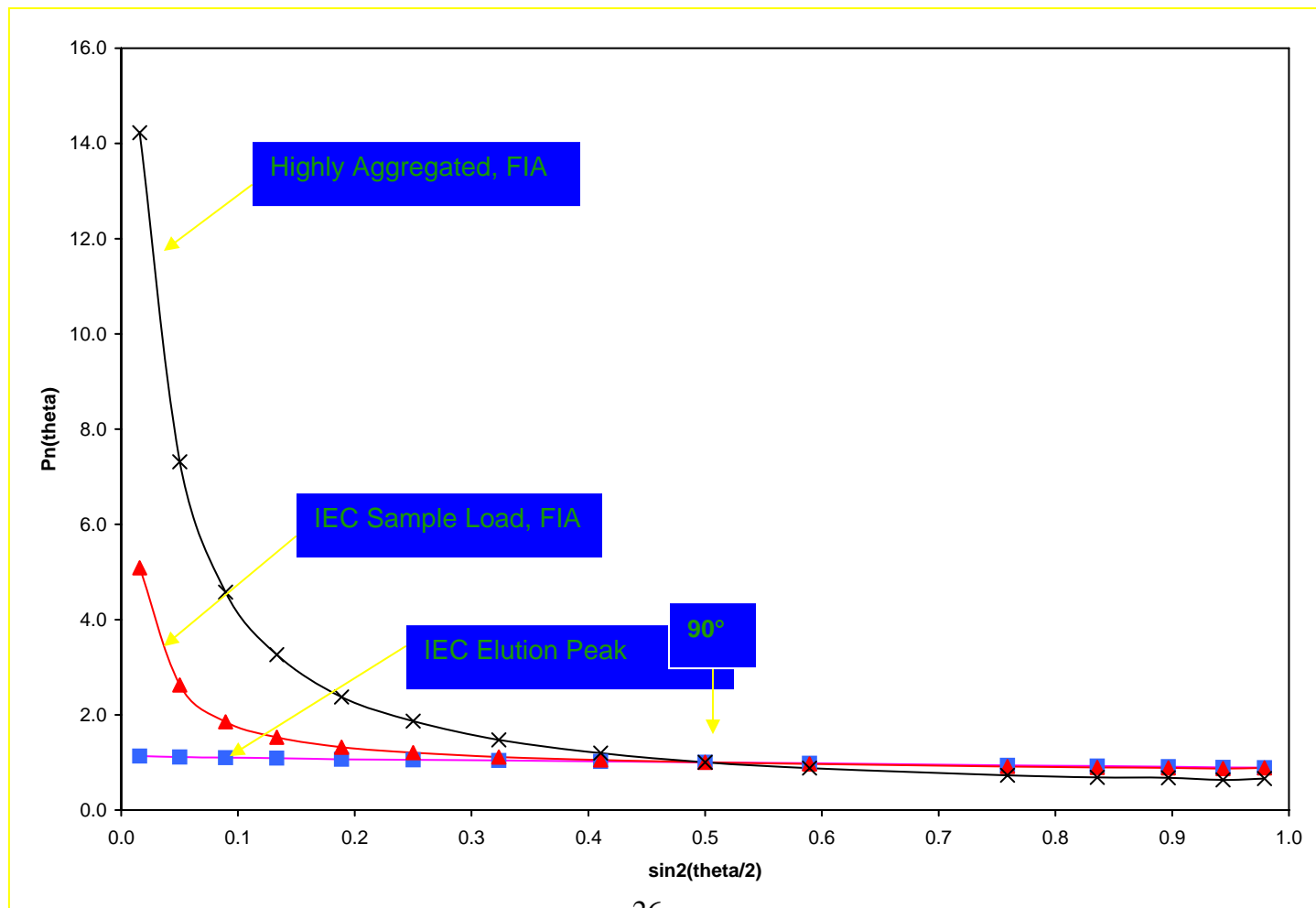


Figure 13 The Effect of 0.5 M Salt on the Normalized LS Envelope of Highly Aggregated Adenovirus

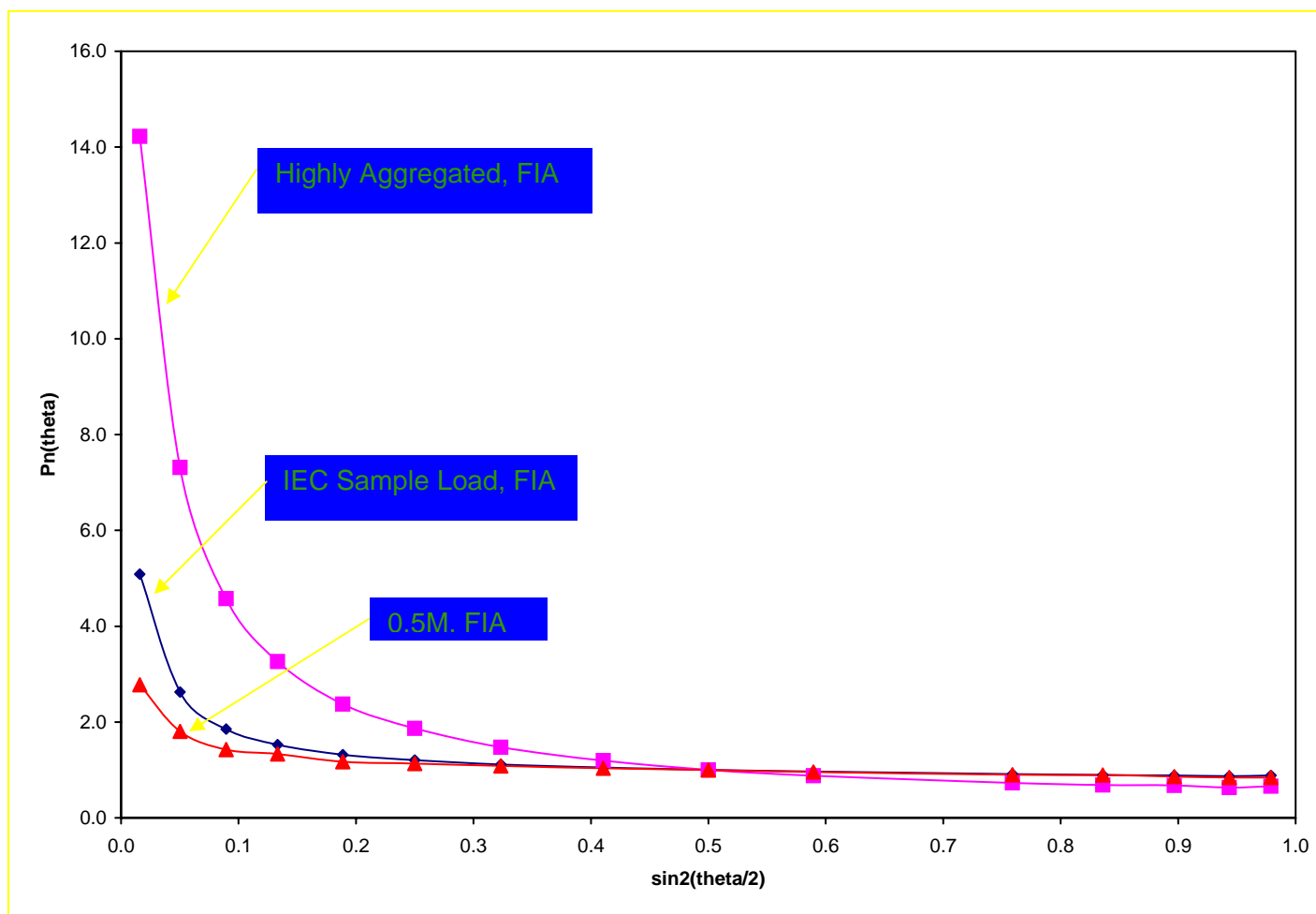


Table 2

Particle Size Information from LS Measurements Conducted during FIA on a Highly Aggregated Lot of Adenovirus and the Effect of Salt on the Observed Aggregation

Sample ID	R _{rms} , nm	R _{eq} , nm	R _h , nm
FIA, high aggregation (flow)	436	565	121
FIA, high aggregation (stop-flow)	397	514	127
FIA, high aggregation + 0.5 M salt (flow)	51	66	59

8. Using the normalized LS envelope, from intensity LS measurements, to assess the polydispersity of an Adenovirus preparation

Although a simple numerical size parameter, such as R_{rms} , can be used to assess the polydispersity of an Adenovirus sample from intensity LS measurements (as is done in the case of DLS using R_h), by determining the limiting slope of the LS envelope at $\theta = 0^\circ$, this process is not straight forward and can be prone to errors due to quality of the data, the range of angles used, how low the angles are, the form of the fitting equation, and the size and polydispersity of the scattering particles. Various numerical methods and equations can be applied to extract this information via computer software analysis. However, these approaches are not universal for all cases. In fact, some approaches are better than others for certain size ranges¹⁰. Because these methods/equations have certain strengths and weakness the finally results can be bias and specific to the method or equation used. Hence one is unsure as to which answer is correct. In addition, the same issues concerning the utility of R_h also apply to R_{eq} . A better approach involves comparing the known LS envelope of the Adenovirus monomer to the experimentally observed LS envelope. This comparison can be simply made by summing the squares of the deviations, SSD, over a defined and fix angle range (the wider and low the angles the better). This can be achieved by subtracting the normalized experimental scattering factors, $P_n(\theta)$ from the normalized theoretical scattering factors of the Adenovirus monomer, $P_n(\theta)_{90nm}$, as shown in eq. 8:

$$SSD = \sum [P_n(\theta)_{90nm} - P_n(\theta)]^2 \quad \text{eq. 8}$$

Hence the lower the SSD value the lower the polydispersity. This approach is simple, removes any bias, and takes advantage of all the raw data without the need to make any decision concerning which equation, angles, or power of the polynomial to use to fit the data. Nevertheless, this approach still does not provide a clear description of the distribution of the Adenovirus aggregates in a given virus preparation.

Part III: The need for other methodologies to evaluate the polydispersity of Adenovirus preparations

Although LS techniques can provide useful data, ***when properly executed***, LS falls short in providing a clear description of the distribution of the particle sizes actually present in a given Adenovirus preparation. Hence other methods need to be investigated to better provide this information. Recently electron microscopy (EM) has been used¹¹, but given the influence the buffer matrix conditions can have on the state of Adenovirus aggregation, as shown in this work, it is not clear what effect the EM sample preparation steps may have in altering the aggregation of the virus sample. The use of other physical chemical techniques, such as field-flow fractionation (FFF)¹² with LS detection and disc centrifugation¹³ have also been investigated. In this study, we have chosen to investigate analytical ultracentrifugation (AUC) as an alternative method. This decision was based on the following:

1. The ability of the AUC to evaluate aggregation over a wide range of particle sizes in the same buffer matrix as the sample.
2. The prior long successful history of AUC in characterizing viruses.
3. The recent new improvements, in term of hardware, software, and methodologies that have greatly improve its capabilities.

In the remaining sections of this presentation, data will be presented which will show the power of the modern AUC to provide information concerning the distribution of monomeric and non-monomeric virus material present in an Adenovirus preparation, as well as other lower molecular weight species, which might correspond to fragments of the virus. In addition, the AUC will also be shown to be capable of providing other important characterization information related to the virus's polydispersity, such as the level of empty capsid material present in these preparations.

An interesting point concerning AUC results is shown in Figure 15. Data in this figure indicates how easy it is for centrifugation, a commonly used clarification step, to remove Adenovirus aggregates. In this case centrifugation at 3000 rpm after only about 15 minute significantly remove virus aggregates.

Part IV: Characterization of Adenovirus by analytical ultracentrifugation (AUC)

1. Sedimentation velocity

Analytical ultracentrifugation analysis using velocity sedimentation offers the direct capability of physically separating the various Adenovirus species present in solution. Combining this separation ability with recent advances in developing software analysis programs, such as SEDFIT¹⁴, has enable the AUC to now provide a rather detailed picture of the distribution of sedimentation coefficients for a given sample. Examples of this type of analysis on Adenovirus samples are shown in Figures 14-16.

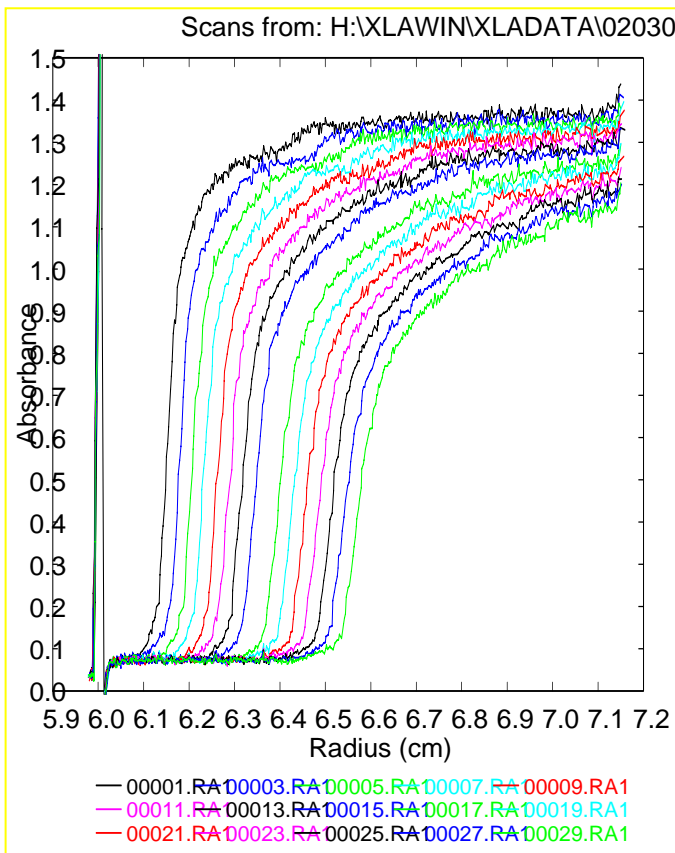
2. Analytical sedimentation equilibrium in a density gradient

Because large amounts of Adenovirus are required for commercial use, the normal laboratory route for purifying this virus by preparative sedimentation equilibrium in a CsCl density gradient is not feasible. Present commercial purification methodology uses ion exchange chromatography. Unfortunately, this simple purification route does not effectively remove empty capsid (virus particles lacking DNA) material, which is normally made during virus production. Hence information on the amount of this material present in Adenovirus preparations as well as additional characterization information concerning the micro-heterogeneity of Adenovirus can be obtained by another AUC technique called analytical sedimentation equilibrium in a density gradient. This technique can characterize the virus in terms of its buoyant density micro-heterogeneity.

Intact Adenovirus particles have a unique chemical composition in terms of the ratio of protein to nucleic acid. Since the buoyant density of proteins and nucleic acids are very different and because sedimentation equilibrium in a density gradient can resolve material with very small difference in buoyant density, this method can provide high resolution information about the density micro-heterogeneity of the virus particles in a given preparation. Results in Figures 17-18 show the ability of the AUC to reveal the different structural forms of Adenovirus present in a virus preparation use this technique.

Figure 14 An Example of Modern AUC Analysis on the Sedimentation Velocity Data Obtained for an Adenovirus Preparation using SEDFIT Computer Program.

A series of UV (260 nm) scans at different times, raw data



Transformation of the entire set of raw data to yield the normalized distribution of sedimentation coefficients, c(s)

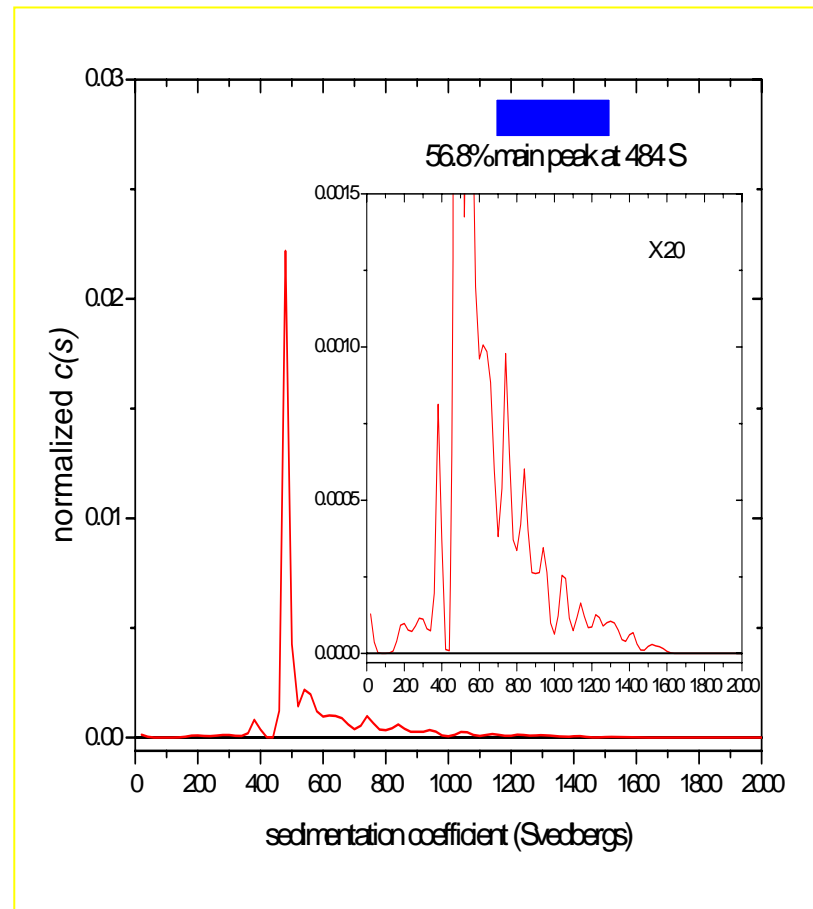
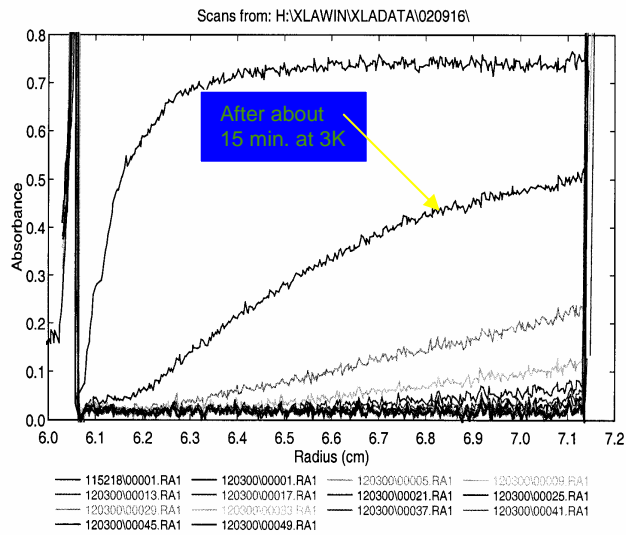


Figure 15 Sedimentation Velocity Data of an Adenovirus Lot Stored at a High Virus Concentration in Formulation Buffer.

This material is composed almost entirely of highly aggregated material having sedimentation coefficient values at 20°C in water, $S_{20,w}$, which approach 200,000 (note: monomeric Adenovirus has an $S_{20,w}$ value of about 750 at infinite dilution).

A) Raw data



B) Resulting normalized distribution of sedimentation coefficients $g(s)$

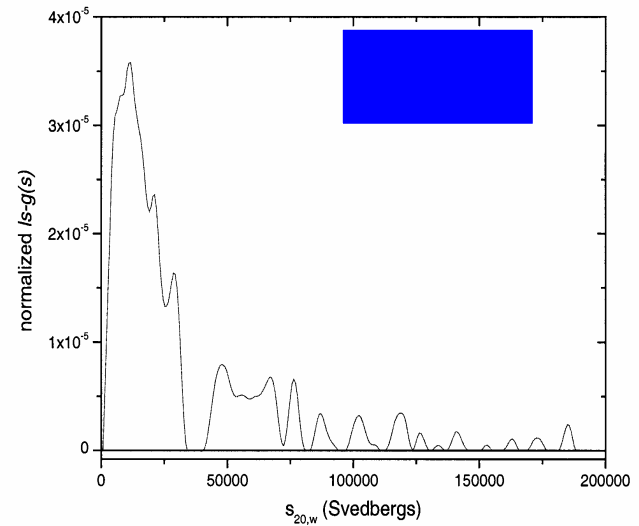
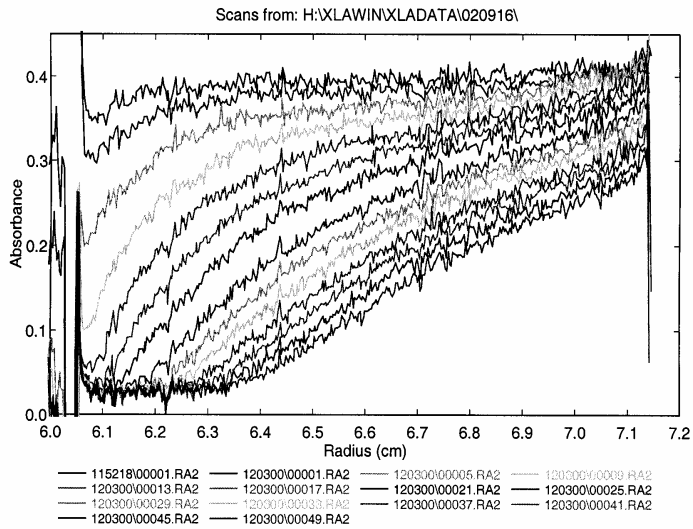


Figure 16 Sedimentation Velocity Data of the Same Adenovirus Lot, but the Buffer Contained 0.5 M NaCl.

This data clearly indicates the disassociating effects of high salt on Adenovirus aggregation induced by high virus concentration and initial low salt.

A) Raw data



B) Resulting sedimentation distribution

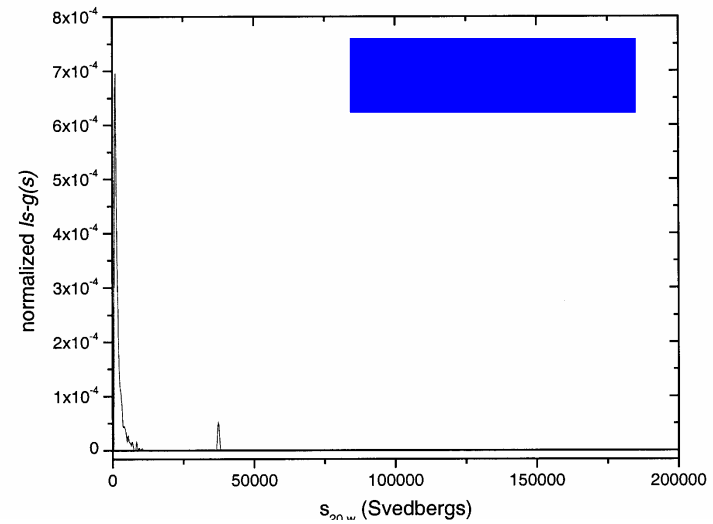
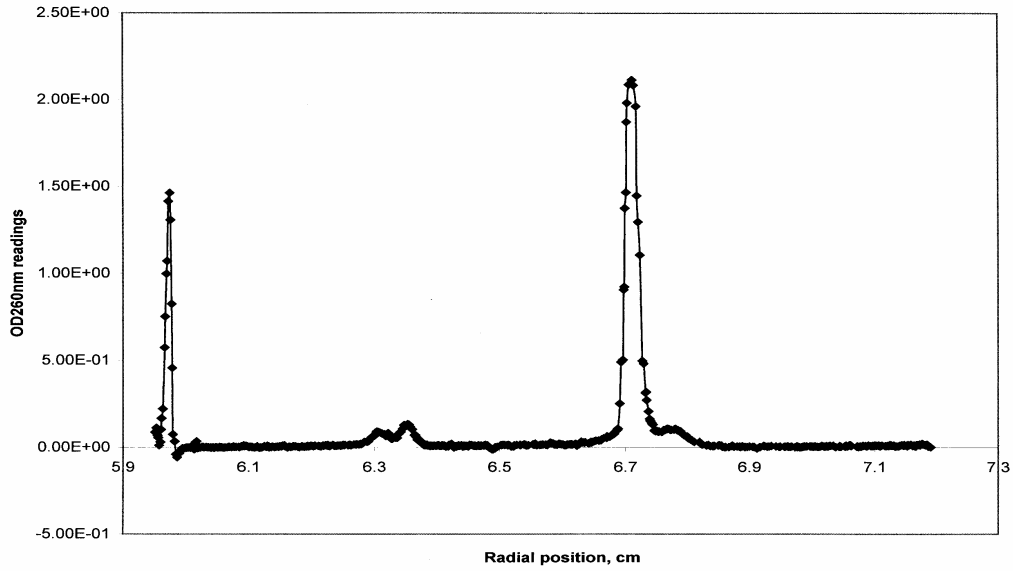


Figure 17 Analytical Sedimentation Equilibrium of an Ion Exchange Purified Adenovirus Lot in a CsCl Density Gradient

A) 260nm UV trace at equilibrium



B) Same sample scanned at 230nm. Peaks I & II could be free protein, empty and nearly empty capsid material?, Peak III is intact virus, Peak IV (virus particles missing protein or containing more DNA?)

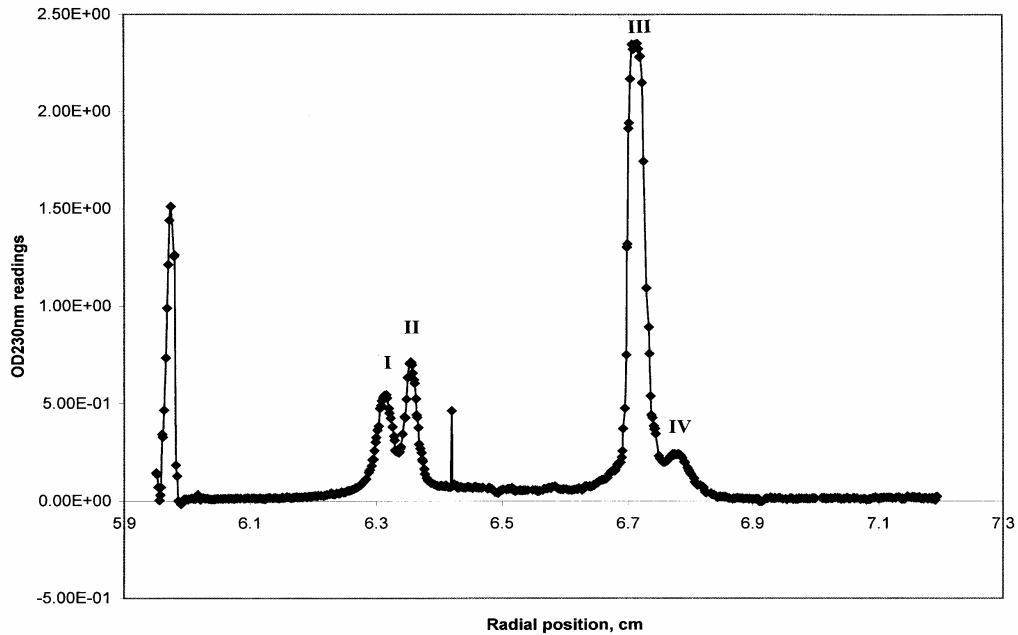
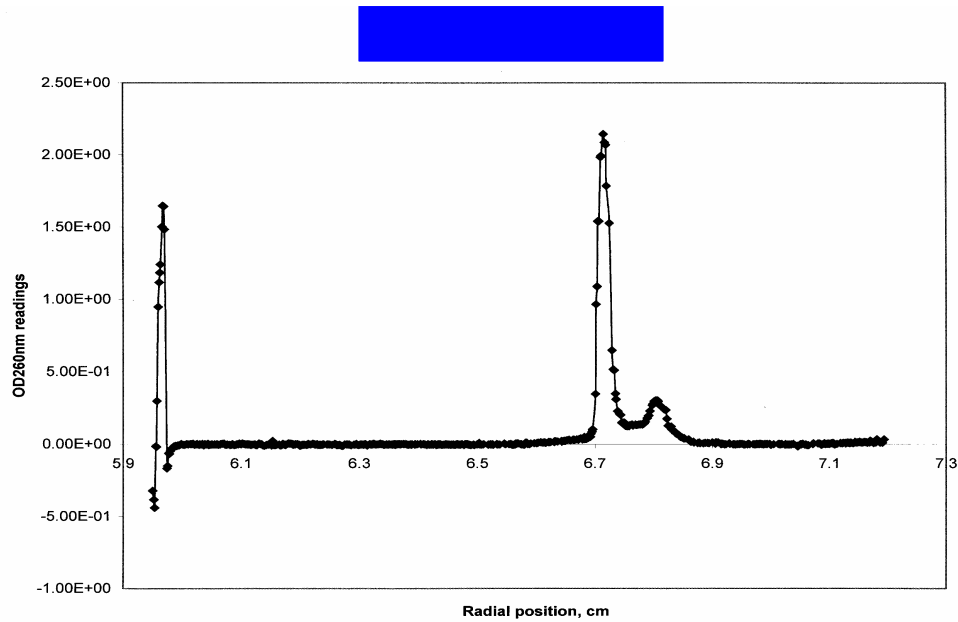
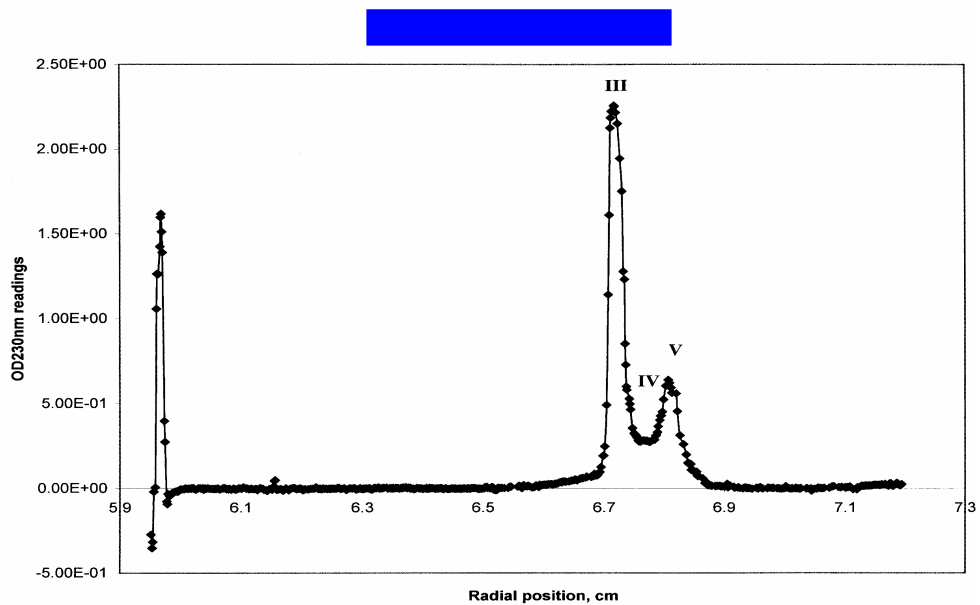


Figure 18 Analytical Sedimentation Equilibrium of a CsCl Purified Lot of Adenovirus in a CsCl Density Gradient.

C) 260nm UV trace at equilibrium (No empty capsid or free protein material detected).



D) Same sample scanned at 230nm. Peak III intact virus, Peaks IV & V (virus particles missing protein or containing more DNA?).



Part V: Conclusion

In conducting LS experiments on Adenovirus, to assess virus aggregation, the following issues must be addressed:

1. Sample clarification processes, normally required for LS experiments, should be avoided since it can remove aggregated virus material, causing the amount of virus aggregation present to be underestimated. Nevertheless without the removal of very large “Dust Particles” problems can exist in obtaining a valid estimate on Adenovirus aggregation by LS.
2. For scatterers the size of Adenovirus aggregates, LS measurements must be conducted over a range of angles that include angles as close to 0° as possible. This is important in order to effectively detect the presence of very large virus aggregates that may be present.

To overcome these issues and to provide more meaningful LS information about Adenovirus aggregation a FIA system, capable of providing HDC, with a LS detector capable of measuring scattered light over a wide range of angles has been used.

Nevertheless, in this study we have demonstrated the ability of the analytical ultracentrifuge to provide a more complete quantitative picture about the distribution of Adenovirus size particles present in a Adenovirus sample. This is due to the well-controlled and defined process of sedimentation, that makes it amenable to rigorous mathematical analysis for extracting particle size distribution information. As a result much more reliable and informative information is generated, which better characterizes the state of aggregation and homogeneity of Adenovirus preparations. This coupled with the AUC's enormous dynamic separation range, enables it to generate effectively more resolution over a wider range of particle sizes (including very low molecular weight material). In addition, alternate modes of separation available to the analytical centrifuge and its ability to run samples in virtually any buffer matrix makes the AUC a powerful and versatile tool for characterizing viruses in terms of its structural homogeneity and state of aggregation.

Part VI: References

1. Kodojo Adadevoh, Maria Croyle Daniel, Daniel Malarme, Edwige Bonfils, Mark A. Bowe, *Bioprocessing*, 1(3), 2002, 62-69.
2. LS measurements made in this study were carried out on either a Wyatt Minidawn or a Wyatt Dawn EOS instrument equipped with a QELS unit.
3. Presentation made at the Wyatt International Light Scattering Colloquium 2002, by Dr. Miles J. Weida from Wyatt Technology Corp.
4. Dennis E. Koppel, *J. of Chem. Phys.*, (1972) 57, 4814-4820.
5. Hamish Small, *Chemtech*, (1977) 7(3), 196-200.
6. Hamish Small, *Anal. Chem.*, (1982) 54, 892A-898A.
7. American Type Culture Collection, Product Information Sheet VR-1516 for the Adenovirus Reference Material (ARM) developed by the Adenovirus Reference Material Working Group (ARMWG).
8. The presence of fiber projections on the Adenovirus could make a measurable contribution to the hydrodynamic properties of the virus leading to an increase in the R_h value relative to the actual radius of the virus capsid.
9. Victor A. Bloomfield, *Biopolymers*, (2000) 54, 168-172.
10. See Wyatt technical Note #10 as well as information provided in their instrument manual for Dawn EOS unit.
11. Linda J. Obenauer-Kutner, Peter M. Ihnat, Tong-Yuan Yany, Barbara J. Dovey-Hartman, Arthi Balu, Constance Cullen, Ronald W. Bordens, Michael J. Grace, *Human Gene Therapy*, (2002) 13, 1687-1696
12. Bruce Mann from Berlex presented FFF results at the CE in the Biotechnology and Pharmaceutical Industries: Practical Applications for the Analysis of Proteins, Nucleotides and Small Molecules 2002 meeting in Washington, D.C.
13. L.L. Bondoc, S. Fitzpatrick, *J. Industrial Microbiology & Biotechnology*, (1998) 20, 317-322.
14. Peter Schuck's web site (<http://analyticalultracentrifugation.com/>) for SEDFIT. A state of the art AUC computer program. This site is loaded with useful information and reference on AUC analysis.